55th Annual Midwest Student Biomedical Research Forum

Saturday, March 2, 2024

ROOM 3040

8:00 a.m. **O-03** TARGETING P38MAPK SIGNALING PATHWAY TO REGULATE TUMOR-ASSOCIATED MACROPHAGE POLARIZATION
Presenter: Daniel Afolabi, Creighton University

8:15 a.m. **O-35** OSELTAMIVIR, A COMMONLY PRESCRIBED INFLUENZA ANTIVIRAL, PROTECTS AGAINST NOISE-INDUCED HEARING LOSS IN A MOUSE MODEL
Presenter: Emma Longsworth, Creighton University

8:30 a.m. **O-54** A STRUCTURE-GUIDED APPROACH TO TARGETING GERANYLGERANYL DIPHOSPHATE SYNTHASE
Presenter: Andrew Pham, UNMC

8:45 a.m. **O-56** ELECTRICAL PULSE STIMULATION PROTECTS C2C12 MYOTUBES AGAINST H_2O_2-INDUCED CYTOTOXICITY VIA ACTIVATING NRF2/ANTIOXIDANT PATHWAY
Presenter Sarah Pribil, UNMC

9:00 a.m. **O-61** TAU EXASPERATES CHRONIC APOE EXPRESSION FOLLOWING TRAUMATIC BRAIN INJURY
Presenter: Nashanthea Roland, UNMC

9:15 a.m. **O-67** MICROGLIA POLARIZE IN RESPONSE TO OCULAR HYPERTENSION DURING GLAUCOMA
Presenter: Jennifer Thompson, UNMC

9:30 a.m. **O-69** TARGETING TREM1-MEDIATED NEUROINFLAMMATION ALLEVIATES GLOBAL ISCHEMIC STROKE PATHOLOGY
Presenter: Rachael Urquhart, Creighton University

9:45 a.m. **O-71** DECIPHERING MECHANISMS OF MITOXANTRONE ACTION IN HR-DEFICIENT CANCER
Presenter: Savanna Wallin, UNMC

10:00 a.m. BREAK

TARGETING P38MAPK SIGNALING PATHWAY TO REGULATE TUMOR-ASSOCIATED MACROPHAGE POLARIZATION

Daniel Afolabi, Venkatlaxmi Chettiar, Peter W. Abel, and Yaping Tu

Department of Pharmacology and Neuroscience, Creighton University School of Medicine, Omaha, NE.

Background and Significance of Problem: Macrophages are a vital component of the immune system that has been widely known to be polarized into either pro-inflammatory and anti-tumor M1 macrophages or anti-inflammatory and pro-tumor M2 macrophages. In a tumor microenvironment, macrophages are recruited and converted to tumor-associated macrophages (TAM), also referred to as M2d macrophages. While both M1 and M2 macrophages are present in the tumor microenvironment, M2-like polarized TAMs increase tumor progression to malignancy and metastasis via angiogenesis, and tissue remodeling and suppress antitumor immune responses. The high influx of TAMs into the tumor correlates with poor clinical outcomes in breast, prostate, ovarian, hepatocellular, and cervical cancers. Thus, TAMs are considered a promising target for novel cancer immunotherapies. However, the molecular mechanisms underlying TAM polarization and the complicated association between TAMs and cancer cells have not yet been clearly elucidated, which hinders the development of TAM-targeted therapy for cancer. Understanding the mechanisms and developing strategies to target TAM polarization pose a significant unmet need.

Hypothesis: The p38 mitogen-activated protein kinase (MAPK) signaling pathway mediates several important inflammatory reactions in response to a variety of stimuli. Recent studies have identified a role for p38 MAPK in IL-4-induced M2 peritoneal macrophage polarization. We hypothesize that targeting the p38MAPK signaling pathway will also regulate tumor-associated macrophage polarization.

Experimental Design: Primary bone marrow-derived macrophages (BMDM) were obtained by in vitro differentiation of mouse bone marrow cells in the presence of macrophage colony-stimulating factor (M-CSF). RAW 264.7 cells are a macrophage-like, Abelson leukemia virus-transformed cell line derived from BALB/c mice. Both mouse BMDM and RAW 264.7 cells were used in our studies. To test our hypothesis, we established two distinct M2d polarization in vitro models: a) Treatment with lipopolysaccharide (LPS) and adenosine analogue NECA for 16 h; b) Treatment with tumor-conditioned medium collected from human A549 or mouse Lewis Lung cancer cells. Morphological analysis and quantitative RT-PCR were performed to assess the M1 and M2 macrophage expression levels with and without different signaling molecule inhibitors. Additionally, a parallel western blot analysis was conducted to examine the protein levels of signaling pathway molecules.

Result: We found that treatment either with 100-500 ng/ml of LPS plus 5 μM NECA or tumor-conditioned medium resulted in M2-specific distinct morphological changes of macrophage cells. M2 marker Arg-1 mRNA and protein levels were also markedly increased upon LPS/NECA or tumor-conditioned medium treatment. Vascular endothelial growth factor (VEGF) promotes tumor progression and metastasis and is produced and secreted by M2d macrophages in the tumor microenvironment. We found that LPS/NECA or tumor-conditioned medium treatment also upregulated VEGF expression in both BMDM and RAW 264.7 macrophages. In the context of signaling molecule inhibitors, Sp1 transcription factor inhibitor decreased both M1 and M2 markers, albeit with a slight reduction in VEGF expression. In contrast, a P38 inhibitor exhibited a decrease in both VEGF and M2 markers in TAM with little or no effect on the M1 markers.

Conclusion: We have successfully established two TAM in vitro models using both primary BMDM and RAW 264.7 cell lines. Importantly, our results showed the significant role of p38MAKP in M2-like TAM polarization. Since inhibition of p38MAKP reduces the M2d macrophages with little effect on M1 macrophage polarization, it may provide a novel approach to target M2-like TAM in cancer progression, thus reducing cancer incidence and cancer-related mortality.

Oseltamivir, A Commonly Prescribed Influenza Antiviral, Protects Against Noise-Induced Hearing Loss in a Mouse Model

Emma Longsworth, Regina Kelmann, Matthew Ingersoll, Richard Lutze, Kristina Ly, Daniel Kresock, Tal Teitz
Department of Pharmacology and Neuroscience, School of Medicine, Creighton University, Omaha, NE, USA

Background: Affecting an estimated 10-15% of all people, noise-induced hearing loss (NIHL) remains a major cause of disability worldwide. Despite this high prevalence, there are no FDA-approved drugs to treat or prevent NIHL, a problem further compounded by the expense and risk associated with the novel drug development process. To circumvent these obstacles, we performed a high-throughput screen (HTS) of previously FDA-approved drugs for protection from cisplatin-induced cell death in an inner ear cell line and identified oseltamivir (Tamiflu), a neuraminidase inhibitor currently approved for the treatment of influenza, as a promising candidate. Oseltamivir was additionally shown to reduce cisplatin-induced hair cell death in an *ex vivo* assay of P3 FVB mouse cochlear explants with low toxicity and high potency, further bolstering its hypothesized otoprotective potential. Given these results, we hypothesized that oseltamivir treatment *in vivo* could mitigate hearing damage following traumatic noise exposure. Moreover, we hypothesized that oseltamivir may be acting as a mammalian neuraminidase inhibitor and opted to test this hypothesis through the use of two additional neuraminidase inhibitors, zanamivir and N-Acetyl-2,3-dehydro-2-deoxyneuraminic acid (DANA), as well as the active form of oseltamivir, oseltamivir carboxylate in cochlear explants.

Methods: Baseline hearing ability was established in 6-8 week old FVB mice through measurements of auditory brainstem response (ABR). Mice were then subjected to a noise challenge consisting of a 2 hour period of exposure to 100 dB SPL noise covering a 8-16 kHz octave band. Twice daily treatment with oseltamivir (10 mg/kg, 50 mg/kg, and 100 mg/kg) or carrier via oral gavage was initiated either 24 or 48 hours following noise exposure and continued for either three or five days. ABR and wave 1 threshold shifts were measured 14 days following treatment. For explant studies, cochlea was collected from P3 pups and treated with zanamivir or DANA along side cisplatin.

Results: Oseltamivir, a high ranking candidate from HTS screening, exhibited low toxicity (TI >220) and high potency (IC_{50} 450 nM) in cochlear explants. *In vivo*, 100 mg/kg oseltamivir treatment significantly protected hearing in noise-exposed mice with an average reduction of ABR threshold shift of 20-25 dB SPL when initiated 24 hours post-noise exposure; no protection was seen when treatment was initiated 48 hours following exposure. Mice treated for five days exhibited no improvement over the three day treatment group. Moreover, oseltamivir-treated mice experienced significant protection of wave 1 amplitude at 80 and 90 dB SPL, as well as counts of Ctbp2 auditory nerve puncta in the 16 kHz region. Results for zanamivir, DANA, and oseltamivir carboxylate in cochlear explants are currently pending.

Conclusions: Oseltamivir emerged as a possible otoprotective compound in our initial HTS and cochlear screens. *In vivo,* oseltamivir treatment rescued multiple indicators of hearing function in mice when given for three days starting 24 hours after traumatic noise exposure, suggesting a window of opportunity for treatment following acoustic trauma. Favorable Ctbp2 auditory nerve puncta counts and wave 1 amplitude results show that oseltamivir treatment protects against measures of cochlear synaptopathy in the setting of traumatic noise exposure. Combined with its widespread availability and regulatory approval, our results suggest oseltamivir is a potential candidate for drug repurposing to prevent noise-induced hearing loss.

A STRUCTURE-GUIDED APPROACH TO TARGETING GERANYLGERANYL DIPHOSPHATE SYNTHASE

Andrew Pham, Lucas Struble, Sarah Holstein, Gloria E.O. Borgstahl
University of Nebraska Medical Center, Omaha NE

Background: Several incurable cancers are characterized by abnormal protein production and secretion. This includes excessive monoclonal protein (MP) secretion in multiple myeloma (MM) due to the proliferation of malignant plasma cells. Aberrant production and secretion of these cancer-related proteins lead to increased disease progression indicated by enhanced metastasis, tumor growth, and drug resistance. As both cancers are incurable and have a high chance of developing drug resistance as the diseases progress, new treatments are highly desirable. Research has shown that inhibition of geranylgeranyl diphosphate synthase (GGDPS) disrupts the function of the intracellular trafficking Rab family of proteins. GGDPS is responsible for synthesizing the 20-carbon isoprenoid group (geranylgeranyl diphosphate or GGDP) from isopentyl pyrophosphate (IPP) and farnesyl diphosphate (FDP). This GGDP group is added to the carboxy terminus of Rab. This addition is essential for Rab's function in intracellular trafficking. Disrupting Rab geranylgeranylation leads to disruption of monoclonal proteins and mucin trafficking resulting in the activation of the unfolded protein response and apoptosis in cancer cells.

Significance of Problem: MM accounts for 10% of all hematological malignancies and is estimated to have affected over 34,000 individuals in the United States in 2021. Of these 34,000 people, over 1/3 are expected to die (12,000). While clinical advancements have been made in treating MM over the years, patients will eventually become either resistant or intolerant to current therapies. Therefore, there is a need to develop new therapeutic strategies targeting this malignancy.

Hypothesis: Our collaborators have synthesized new potent inhibitors with high specificity for GGDPS. Interestingly, stereoisomers of these inhibitors exhibit low IC50s individually but demonstrate even lower IC50s when mixed. We hypothesize that one stereoisomer binds to the GGDP product site while the other stereoisomer binds to the FDP substrate site. We hope to use this knowledge to further assist in structure-based GGDPS drug design.

Experimental Design: To answer how these stereoisomers differentially bind GGDPS, we will use crystallography to solve the structure of our protein bound by these inhibitors. We first express His-tagged GGDPS in BL21 DE3 *E. coli* followed by purification through nickel affinity and size exclusion. Proteins go through the dynamic light scattering machine to check for monodispersity and 96-wells are set up to screen for crystallization conditions. Crystals hits are then optimized in a 24-well. Once a crystallization condition is found that readily crystallizes our protein, we will ligand soak or crystals or co-crystallize our proteins with drug.

Results: We were able to screen and obtain an initial condition that grew microcrystals (~50 µm diameter). Prior trips to the national synchrotron showed diffraction was possible up to 4 Å. These crystals were further optimized by using more pure reagents. This led to crystal growth in a shorter amount of time and of larger size (~100 µm diameter). Additionally, we were able to grow larger crystals utilizing a micro batch under-oil method. These crystals grew between 1 to 3 months. Our upcoming data collection trips will be using crystals that grew both larger and cleaner from recent experiments. Differential scanning fluorimetry (DSF) has confirmed the drug stereoisomers to bind GGDPS at a 2:1 molar ratio. Negative stain electron microscopy reveals GGDPS does not aggregate when co-incubated with these drugs, making GGDPS a good candidate for potential cryo-EM experiments in the future.

Conclusion: GGDPS microcrystals were reliably obtained overnight in 0.1 M salt and 12% PEG. Crystals grown in 0.1 M salt and 20% to 30% PEG utilizing an under-oil method of crystallization grew cleaner crystals but took much longer (1 to 3 months). These crystals could be co-crystallized with each stereoisomer individually as well as together. Crystals from both these conditions will be brought to the national synchrotron for data collection. DSF showed that both stereoisomers could bind GGDPS at a 2:1 drug to protein ratio. Negative stain electron microscopy confirms GGDPS to not aggregate in solution when co-incubated with these compounds revealing a favorable preliminary result for cryo-EM experiments.

ELECTRICAL PULSE STIMULATION PROTECTS C2C12 MYOTUBES AGAINST H_2O_2-INDUCED CYTOTOXICITY *VIA* ACTIVATING NRF2/ANTIOXIDANT PATHWAY

Sarah Pribil[1], Anjali Bhat[1], Cody Anderson[2], Will Bruening[1], Joel Jacob[1], Ved Vasishtha Pendyala[1], Li Yu[1], Taylor Bruett[3], Matthew Zimmerman[3], Song-Young Park[2], Lie Gao[1]

[1]Department of Anesthesiology, University of Nebraska Medical Center, Omaha, NE
[2]School of Health and Kinesiology, University of Nebraska Omaha, Omaha, NE
[3]Department of Cellular and Integrative Physiology, University of Nebraska Medical Center, Omaha, NE

Background: In response to various physiological stimuli during exercise, skeletal muscle (SkM), a highly plastic tissue, is capable of functional and structural remodeling. A previous study by our laboratory (Ref 1) demonstrated that chronic exercise training significantly upregulated a large group of antioxidant enzymes in SkM *via* activating nuclear factor-erythroid factor 2-related factor 2 (Nrf2), a master transcription factor responsible for intracellular redox hemostasis. However, the underlying mechanisms are unknown, and the functional significance remains to be determined.

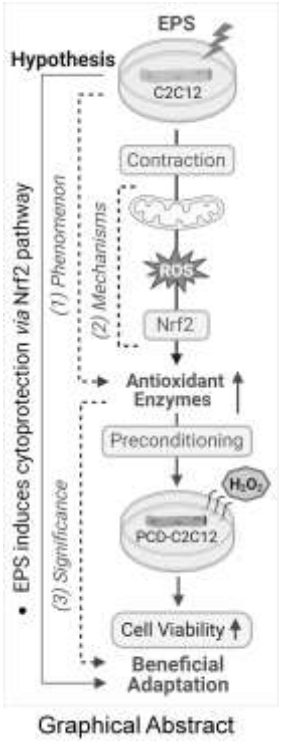

Graphical Abstract

Significance of the Problem: It is known that exercise has protective effects on various organs and tissues throughout the body; however, the mechanisms which underly this phenomenon are not yet understood. This study aims to elucidate the mechanism(s) by which contracting SkM can protect itself against reactive oxygen species (ROS)-induced cytotoxicity.

Hypothesis: Reactive oxygen species (ROS) play a critical role in contraction-induced activation of the Nrf2/antioxidant system, which, in turn, protects skeletal myotubes against subsequent oxidative-stress cytotoxicity.

Experimental Design: The study was carried out in an *in vitro* contraction model using C2C12 myotubes. The myotubes were plated at 50,000 cells/well in a 6-well plate where they underwent electrical pulse stimulation (EPS) at 10 V, 10 ms, 50 Hz, 0.3 sec/3 sec for 1 hour/day for 4 days.

Results:

(1) By completing experiments for time-course (0 – 6 days) and dose-effect (0 – 10 voltage) to optimize EPS parameters, we found that NQO1 and GSTA2 proteins, two well-known targets of Nrf2, were maximally upregulated with 3.3- and 12.1-fold increase by an EPS at 10 voltage for 4 days. Therefore, these parameters were used in the following experiments.

(2) MitoSOX-Red, CM-H2DCFDA, confocal microscopy, and electron paramagnetic resonance (EPR) assay revealed significantly higher ROS levels in mitochondria, cytosol, and the whole cell of EPS-cells than control-cells. Western blot data suggests that EPS-cells express significantly higher Nrf2 and a broad array of downstream antioxidant enzymes (SOD1, SOD2, Cat, GPX, NQO1, GSTA2, GSTA4, PRX1, and TRX). This phenomenon was completely abolished by pretreatment with N-acetylcysteine, a ROS scavenger. These data suggest that contraction enhances muscle antioxidant defense through ROS-dependent, Nrf2-activated, multi-antioxidant mechanisms, including the first line antioxidant components, glutathione system, thioredoxin system, and peroxiredoxin system.

(3) Seahorse and Oroboros assays found that EPS significantly increased mitochondrial basal and maximal oxygen consumption rate and ATP-linked respiration, along with a significantly upregulated protein expression of mitochondrial complexes I/V (CI and CV), mitofusin-1 (MFN1), and mitochondrial fission factor (MFF). This suggests an enhanced mitochondrial function and biogenesis.

(4) A post-stimulation time-course experiment demonstrated that EPS-induced upregulation of NQO1 and GSTA2 protein expression lasted at least 24 hours after ceasing the stimulation. This suggests that EPS induces an antioxidant preconditioning on these cells, which may protect them against subsequent oxidative stress.

(5) A cell viability study using CCK-8 assay demonstrated that EPS-cells displayed 10.8- and 36.2-fold higher survival rate than the control-cells in response to 2 and 4 mM H_2O_2 treatment, suggesting that EPS bestows these skeletal myocytes with an enhanced antioxidant capacity.

Conclusion: We found that EPS dramatically upregulated a large group of antioxidant enzymes in C2C12 myotubes, which exhibit an increased mitochondrial function and enhanced tolerance to oxidative challenge. These data suggest that contraction can evoke antioxidant adaptation in muscle *via* mitochondrion-ROS-Nrf2 pathway, which provides myocytes with protection against subsequent oxidative stress-associated cytotoxicity.

Reference (1): Bhat A, Abu R, Jagadesan S, Vellichiramal N, Pendyala V, Yu L, Rudebush TL, Guda C, Zucker IH, Kumar V, Gao L. Quantitative Proteomics Identifies Novel Nrf2-Mediated Adaptative Signaling Pathways in Skeletal Muscle Following Exercise Training. Antioxidants. 2023;12:151. https://www.mdpi.com/2076-3921/12/1/151. PMID: 36671013.

TAU EXASPERATES CHRONIC APOE EXPRESSION FOLLOWING TRAUMATIC BRAIN INJURY

Nashanthea Roland, Jane Mattingly, Lexi Sheldon, Joseph George, and Kelly Stauch
University of Nebraska Medical Center, Omaha, Nebraska

Background

Traumatic brain injury (TBI) is the most common cause of long-term disability worldwide. A key pathological characteristic of TBI is the aggregation of hyperphosphorylated tau at the injury site and its propagation to adjacent regions. Tau pathology is also a crucial component in Alzheimer's disease pathogenesis with the progression of the neurodegenerative disease corelating with the extent of pathologic tau accumulation. Another key factor in TBI is prolonged gliosis in AD-relevant brain regions (hippocampus and cortex). This chronic pro-inflammatory immune response, mediated by microglia and astrocytes, is a main contributor to the long-term detriments that plague TBI patients for many years after the initial injury. Activated glia can lead to further neurodegeneration through the exaggerated engulfment of neuronal compartments.

Significance of Problem

TBI outcome can manifest in different ways and can continue to cause issues for individuals for many years after the initial injury. In many cases, chronic glial activation is a profound factor that causes more harm than good. Understanding the role of gliosis in the context of TBI outcome and TBI-induced tau pathology will uncover potential therapeutic targets for more effective treatment. Additionally, most groups in the TBI field have only evaluated acute and subacute endpoints (1 day and up to 3 weeks, respectively). Here, we have done a 30-day post injury (dpi) endpoint.

Question

Considering that there is a plethora of neuroinflammatory genes and pathways affected by TBI, not much is known about the involvement of tau pathology in this context. Therefore, *how is the presence of human tau affecting glial response and activation in AD-relevant brain regions 30 days following TBI?*

Experimental Design

Male and female WT and hTau mice, mice expressing all six isoforms of human tau without murine tau, were subjected to controlled cortical impact surgeries at 2 months of age. Parameters were set to simulate a mild to moderate injury (speed-3.5 m/s, dwell time-0.2 s, depth-0.5mm). Following the initial injury, pioglitazone (10 mg/kg/injection), a PPAR gamma agonist that inhibits glial activation, or vehicle was administered 30 minutes after the initial injury and every 24 hours for five consecutive days (six treatments total). These mice were then sacrificed 30 dpi and used for either histological assessment or biochemical assays. RNA was extracted from the ipsilateral hippocampus and used for NanoString Neuroinflammatory panel analysis and quantitative RT-PCR to validate target genes that were differentially expressed after nSolver analysis. Brain hemispheres were taken and fixed in preparation for histology where Dual RNAScope – ISH IHC was used to assess cell- and region-specific target gene expression.

Results/Data

The NanoString Neuroinflammatory panel showed more differentially expressed genes (upregulated) in hTau TBI mouse ipsilateral hippocampus compared to that of WT and hTau Sham controls. Although the effect was dampened by pioglitazone treatment, the number of differentially expressed genes was still greater in hTau mice compared to that of WT. To validate some genes that were significantly upregulated in hTau mice (even after pioglitazone treatment), but not WT, we used qRT-PCR analysis. We found that *ApoE* and *Trem2* were still highly upregulated in hTau TBI mice with no significant differences between injury groups for WT. RNAScope assessment showed that while astrocytes were the primary producers of *ApoE* in the hippocampus (dentate gyrus, CA1, and CA3), microglia seemed to play a larger role in *ApoE* expression in the cortex and the thalamus. The region-specific *ApoE* expression was more dependent on the injury than human tau expression.

Conclusions

TBI induces increased *ApoE* gene expression in hTau mice which was shown by bulk hippocampal NanoString data and qRT-PCR validation. With the addition of pioglitazone, astrocytic *ApoE* expression continued to be upregulated in the hippocampal regions in both WT and hTau TBI mice 30 dpi. However, microglia were the cells expressing *ApoE* in the thalamus revealing region-specific cell-type expression of *ApoE* following TBI regardless of human tau expression and pioglitazone treatment. APOE polymorphic alleles are the main genetic determinants of AD risk, providing a link between tau, TBI, and subsequent AD.

Microglia Polarize in Response to Ocular Hypertension during Glaucoma

Jennifer Thompson[1,2], Jennie C. Smith[2], Shaylah McCool[1,2], Shan Fan[2], Carol Tores[2,3], Matthew Van Hook[1,2]
University of Nebraska Medical Center, Omaha NE, USA, [2]Truhlsen Eye Institute, Omaha NE, USA [3]The Ohio State University, Columbus, OH, USA.

BACKGROUND: Primary open angle glaucoma (POAG) is an age-related neurodegenerative disorder of the visual system that is projected to affect 74.6 million people worldwide by 2025 (Kapetanakis et al., 2016). Prolonged or untreated glaucoma eventually leads to blindness through the selective and irrecoverable loss of retinal ganglion cells (RGCs)- the only neurons able to transmit visual information from the eye to the brain. To date, high eye pressure (ocular hypertension; OHT) is the only-known modifiable risk factor for glaucoma, yet the mechanism through which elevated IOP (intraocular pressure) contributes to RGC dysfunction and, ultimately death, has not been fully elucidated. In OHT-associated POAG, visual brain regions experience synaptic changes well in advance of neuronal death, including a reduced number of presynaptic input to retinorecipient neurons. Throughout visual system development, some RGC-inputs are selectively targeted for microglia-mediated elimination, and it is possible that similar mechanisms enact to remove presynaptic terminals during glaucomatous neurodegeneration. Therefore, we have asked whether chronic OHT primes microglia/macrophages to aberrantly eliminate RGC-inputs within the visual thalamus (dorsolateral geniculate nucleus; dLGN) during glaucomatous neurodegeneration. ***Significance of Problem:*** There is an urgent unmet need to identify the means by which RGCs are lost in glaucoma, especially at the presynaptic compartment, which is susceptible to dysfunction and degeneration prior to the initiation of apoptotic events at the level of the retina. Exposing mechanisms of synaptic loss in the glaucomatous brain may uncover novel targets for neuroprotective therapies. ***Hypothesis:*** We hypothesize that chronic OHT predisposes RGC axon terminals in the dLGN to microglia-mediated elimination by polarizing microglia/macrophages towards a phagocytic state.

EXPERIMENTAL DESIGN: Here, we used a mouse model of inherited OHT (DBA/2J; D2) to investigate the morphology of microglia/macrophages (Iba1+ cells) in the dLGN at timepoints corresponding to pre- (4m), early- (9m), and progressive glaucoma (12m); a strain-matched control (DBA/2J^{Gpnmb+}; D2-Control) that does not develop OHT was used for comparisons. During the living phase, we took monthly IOP measurements using a rebound tonometer. Following sacrifice, fixed tissue from central regions of the dLGN were immunolabeled with an antibody against Iba1 (ionized calcium-binding adaptor molecule 1) in order to analyze the morphology of microglia/macrophages with a skeletonization protocol. To investigate retinal innervation, we quantified RGC axon terminals that were positively labeled by an antibody against vesicular glutamate transporter 2 (vGlut2+). To explore the possibility that presynaptic RGC terminals might be tagged for elimination in a process similar to development, we used an antibody against C1q (complement component 1q) and quantified signal intensity within the central dLGN. Similar to humans, the nonhuman primate (NHP) visual thalamus is organized into eye-specific anatomical layers. Therefore, in addition to our mouse studies, we sought to repeat our histological approach using brain tissue from a Rhesus macaque that had been the subject of left-eye experimental glaucoma (laser-induced ocular hypertension; see: Sosnowik et al., 2022). Using coronal sections stained by H&E, we segmented the magno- and parvocellular layers of the right and left LGN and quantified layer-specific area fractions. We used 50µm-thick coronal sections to fluorescently-label microglia/macrophages (anti-Iba1), then acquired tile-scans of z-stacks across the entire LGN of each hemisphere. Within each layer, Iba1+ cells were traced by hand along each plane, then the 3-D cell was binarized and reduced to a one-pixel dimension for individual skeleton analysis.

RESULTS/DATA: The D2 dLGN had an IOP-dependent reduction in vGlut2+ density ($R^2 = .313$; $p < 0.001$; $n = 39$), while no age- or IOP-dependent vGlut2+ loss could be detected in controls ($p = 0.703$; $p = 0.817$; $n = 36$). C1q intensity analysis (D2, n=25; D2-C, n=22) revealed that C1q expression in the D2 dLGN increased by 9- and 12m; this increase was IOP-dependent ($R^2 = 0.384$; $p < .001$) and associated with vGlut2+ loss ($R^2 = .304$; $p = .0011$). Pre-glaucoma C1q expression in D2s was consistent with the low, unchanging levels that we observed at all timepoints for controls ($p = .277$). Regarding the presence and morphology of Iba1+ cells, results from global skeleton analyses revealed negative associations between OHT and features of Iba1+ cell ramification, with IOP explaining ~ 30% of arborization variability ($R^2 = 0.298$, $p < .0001$) and 26% of endpoint variability ($R^2 = 0.263$, $p < .0001$). Additionally, we highlight correlations between microglia morphology, loss of RGC terminals, and elevated C1q expression in DBA/2J glaucoma. In NHP glaucoma, we found glaucoma-associated LGN layers had reduced area fractions in side-by-side comparisons to the non-glaucomatous contralateral layer. Results from individual skeleton analyses showed that Iba1+ cells within the glaucomatous P3 layer had significantly fewer branches and endpoints per cell, similar to the morphological changes we observed in DBA/2J glaucoma.

CONCLUSIONS: In mouse and nonhuman primate glaucoma, we have demonstrated that microglia/macrophages in the dLGN exhibit a characteristic response OHT, which involves a reduction in branching and points of contact. Further, the loss of RGC-input to the dLGN and concomitant rise in C1q observed in DBA/2J glaucoma, lend support to our hypothesis that complement-mediated processes may be participating in RGC synapse removal during glaucomatous neurodegeneration.

REFERENCES:

Kapetanakis, V. V., Chan, M. P. Y., Foster, P. J., Cook, D. G., Owen, C. G., & Rudnicka, A. R. (2016). Global variations and time trends in the prevalence of primary open angle glaucoma (POAG): A systematic review and meta-analysis. *British Journal of Ophthalmology*, *100*(1), 86–93. https://doi.org/10.1136/bjophthalmol-2015-307223

Sosnowik, S., Swain, D. L., Fan, S., Toris, C. B., & Gong, H. (2022). Morphological changes to Schlemm's canal and the distal aqueous outflow pathway in monkey eyes with laser-induced ocular hypertension. *Experimental Eye Research*, *219*, 109030. https://doi.org/10.1016/j.exer.2022.109030

TARGETING TREM1-MEDIATED NEUROINFLAMMATION ALLEVIATES GLOBAL ISCHEMIC STROKE PATHOLOGY

Rachael Urquhart, Hyunha Kim, Gopal P Jadhav, and Jee-Yeon Hwang
Creighton University, Department of Pharmacology & Neuroscience, Omaha, NE

Global cerebral ischemia occurs when blood flow to the entire brain is blocked and is most often associated with cardiac arrest. Global ischemia induces delayed, selective hippocampal CA1 pyramidal neurodegeneration, leading to impaired learning and memory. Current therapies for cardiac arrest focus acutely on cardiac function and blood flow – no treatments prevent the chronic, long-term effects of global ischemia. Thus, identifying the molecular mechanisms underlying global ischemia pathology is essential for developing novel treatments to prevent global ischemia-induced neuronal death and cognitive deficits.

In this study, we sought to explore how dysregulation of genes might promote the neurodegeneration associated with global ischemia. Toward this end, we subjected rats to global ischemia via 4-vessel occlusion (4-VO) and performed RNA-seq to investigate alterations of mRNAs in post-ischemic CA1. Ingenuity Pathway Analysis revealed that 'neuroinflammation' and 'TREM1 signaling' are among the top canonical pathways upregulated following global ischemia. TREM1 is a myeloid-derived surface receptor involved in immunity and inflammation with known roles in myocardial ischemia and sepsis, but the role of TREM1 in neuroinflammation and global ischemia remains unclear. Based on our RNA-seq analysis, we hypothesized TREM1 mediated neuroinflammation drives global ischemia induced neuronal death and cognitive deficits, and TREM1 inhibition attenuates this pathology. To address this, we performed RT-qPCR and Western blot analyses which revealed increased TREM1 expression within 48HR , and differential expression of downstream inflammatory cytokines and transcription within 3-48HR post 4-VO. These results validate RNA-seq and IPA, confirming that TREM1 signaling is activated after global ischemia. Cytokine profiling also revealed proinflammatory cytokines related to memory-associated synaptic plasticity (CX3CL1) were decreased, while those related to leukocyte recruitment, blood-brain barrier (BBB) breakdown, and inflammation (ICAM-1, CXCL7, VEGF) were increased within 3-24HR after global ischemia. Taken together, these data establish that TREM1-mediated neuroinflammation takes place in the hippocampal CA1 following global ischemia.

Next, to examine the cell type in which TREM1 is activated after global ischemia, we performed IHC using various cell type markers. TREM1 is localized in CD11b+ immune cells (myeloid cells and microglia) but not in NeuN+ neurons or GFAP+ astrocytes in hippocampal CA1 region at 24 h after global ischemia *vs.* sham. In addition, TREM1 is not observed in Iba1+ ramified microglia at 24 h, indicating that microglia is not activated within 24 h after ischemia and TREM1 is not localized in resting microglia. These results suggest that TREM1 may have its action in the brain due to peripherally infiltrating immune cells. To further explore this, BBB integrity following global ischemia was assessed via IHC, revealing a temporal increase in CD31 and IgG immunofluorescence within and dispersing from the hippocampal CA1 following 4-VO. This increase in CD31 and IgG, a blood circulating antibody, indicates deterioration of the BBB, which may allow the infiltration of CD11b+TREM1+ cells. IHC also revealed a concomitant increase in microglial marker Iba-1 and decrease in neuronal marker NeuN respectively at 72 h and 7 d after ischemia, suggesting that both microglial activation and neurodegeneration occur in the CA1 in response to global ischemia.

To establish a causal relationship between TREM1 and global ischemia, the effect of TREM1 inhibition via the LR12 peptide was measured. LR12 administration reduced neurodegeneration in the hippocampal CA1 after ischemia, measured by histological staining. Western Blot analyses also revealed that when LR12 was administered once per day over a 48HR period, protein expression levels for TREM1 and downstream targets appear decreased. Data regarding the effect of LR12 on BBB integrity and microglial activation has been collected and is currently undergoing analysis.

Overall, this research aims to establish the role of TREM1-mediated neuroinflammatory signaling in global ischemia pathology and identify TREM1 as a potential therapeutic target for attenuating global ischemia-induced neurodegeneration and cognitive deficits.

DECIPHERING MECHANISMS OF MITOXANTRONE ACTION IN HR-DEFICIENT CANCER

Savanna Wallin, Gloria E. O. Borgstahl, Eppley Institute For Research in Cancer and Allied Diseases, University of Nebraska Medical Center, Omaha, NE.

Background and Significance

Genomic instability is a hallmark of cancer and is incited by DNA damage. Sources that instigate genomic instability include exogenous and endogenous DNA-damaging agents, as well as mutated DNA repair proteins that perform inadequately. For instance, deficiencies in the DNA repair pathway homologous recombination (HR) are associated with ovarian, breast, and pancreatic cancers. HR is essential for the error-free repair of double-stranded breaks (DSBs) in DNA, the most harmful form of DNA damage. Cells deficient in HR typically have mutations or deletions in proteins such as BRCA1, BRCA2, or PALB2, and they are dependent on RAD52 to maintain genomic stability. The literature has demonstrated that RAD52 is a promising drug target because RAD52 inhibition in HR-deficient cancer cells causes synthetic lethality. Previous research by our lab has identified several hit compounds capable of inhibiting the RAD52:RPA protein-protein interaction (PPI), a complex critically important early in the HR pathway. One of these hits was identified as Mitoxantrone (MX), an FDA-approved anticancer therapeutic originally approved to treat acute myeloid leukemia. The discovery was striking because even though MX has been used in oncology clinics since the 1980s, its interaction with the RAD52:RPA protein-protein interface was previously unknown. Recent studies have uncovered additional cellular targets of MX and its effects on transcription, highlighting the limited understanding of this commonly used cancer drug. Therefore, there is an urgent need to define the comprehensive molecular and proteomic profile of MX to understand its full therapeutic potential. **We hypothesize that understanding the molecular targets and mechanisms of MX is integral to expanding its therapeutic potential and providing the necessary information to guide future drug design.**

Experimental Design

The FluorIA (fluorescence-based protein-protein interaction assay) identified MX as an inhibitor of the RAD52:RPA PPI. To further explore this interaction and better describe a novel mechanism of action for MX in HR-deficient cancer, we quantified the binding kinetics and assessed the biophysical interaction of MX and RAD52 using surface plasmon resonance (SPR) and limited proteolysis. We also used a biotinylated-mitoxantrone probe (MXP) to characterize cellular binding partners in cell extract, and to validate MX's interaction with RAD52 and rule out RPA interaction.

Results

After identifying MX as an inhibitor of the RPA:RAD52 complex with the FluorIA, we used SPR to determine its affinity for RAD52. MX showed a modest interaction with a dissociation constant (K_D) of 60 μM. We assessed the biophysical nature of this interaction using limited proteolysis which demonstrated that MX stabilizes RAD52 and protects it from proteolytic degradation. Lastly, we tested MXP in different cell lysates and confirmed its interaction with RAD52 by detecting RAD52 in the fraction eluted from the probe via western blot.

Conclusions

The initial identification of MX in the FluorIA led us to investigate this previously unknown interaction with RAD52. Even though MX has been used in the clinic as an anticancer therapeutic for decades, it is exciting to re-examine it through a new lens, which may extend its application in HR-deficient cancer. From the literature and our data, it is clear that MX's mode of action is multi-faceted and has complex interactions within the cell. Our future crystallographic and proteomic analyses will offer specific details into the mechanistic inhibition of RAD52 by MX and define its complete proteomic profile, which will provide critical information for future structure-guided drug design.